Journal of Photochemistry and Photobiology A: Chemistry 214 (2010) 269–275

Contents lists available at ScienceDirect

Journal of Photochemistry and Photobiology A: Chemistry

journal homepage: www.elsevier.com/locate/jphotochem

Substituent effect in direct ring functionalized squaraine dyes on near infra-red sensitization of nanocrystalline TiO_2 for molecular photovoltaics

Shyam S. Pandey[a,*], Takafumi Inoue[a], Naotaka Fujikawa[a], Yoshihiro Yamaguchi[b], Shuji Hayase[a]

[a] Kyushu Institute of Technology, 2-4 Hibikino, Wakamatsu, Kitakyushu 808-1096, Japan
[b] Nippon Steel Chemical Company Limited, Nakabaru, Tobata, Kitakyushu, Japan

ARTICLE INFO

Article history:
Received 9 March 2010
Received in revised form 3 June 2010
Accepted 8 July 2010
Available online 16 July 2010

Keywords:
Dye-sensitized solar cells
Aggregation
Surface passivation
Squarine dyes
Nanocrystalline TiO_2

ABSTRACT

We have synthesized a series of novel blue colored symmetrical squaraine sensitizers with variable alkyl chain length for their application towards the fabrication of dye-sensitized solar cells (DSSCs). It has been found that an increase in the alkyl chain length substituted at N-position of indole ring exhibits enhanced electron diffusion length and electron life-time resulting in better passivation of nanocrystalline TiO_2 surface leading to enhancement in the cell performance. Based on HOMO and LUMO energy measurement of squaraine dyes, it has been demonstrated that about 0.16 eV energy barrier is sufficient for electron injection from LUMO of dye to TiO_2 conduction band and dye regeneration after photo-excitation. Performances of DSSCs using model squaraine dyes indicate that dodecyl alkyl substituent is optimum giving highest Voc and use of chenodeoxycholic acid along with the dye **SQ-4** shows a photoconversion efficiency of 3.5% under AM 1.5 irradiation.

1. Introduction

A new paradigm in harnessing the immense solar energy driven by cast and quality has attracted the attention of material scientists in the recent past. Report of conversion efficiency over 10% by ruthenium based dye-sensitized solar cells (DSSCs) has brought up new momentum in the energy research [1,2]. A perusal of absorption spectrum of ruthenium sensitizers and solar spectrum clearly indicates a need for novel sensitizers absorbing in near infra-red (NIR) wavelength region for further enhancement in the photoconversion efficiency. Recently, there are reports about the extension of optical absorption window associated with photon harvesting in the wide wavelength region by selective adsorption of two dyes in dye double architecture leading to the enhancement in the conversion efficiency [3,4]. Our approach is to develop NIR sensitizers and fabricate the efficient DSSCs by combining them with ruthenium based sensitizers in dye double layer architecture. In this regard, squaric acid based dyes are one of the potential candidates owing to their intense sharp absorption in NIR region, high molar extinction coefficient and their stability along with application as sensitizers in the xerography and optical data storage [5,6]. At the same time, optical absorption of such dyes are possible to tailor in extended wavelength region by the judicious selection of aromatic donor moieties with extended π-conjugation surrounding the electron deficient squaric acid central core [7].

Yum et al. [8] have reported an unsymmetrical squaraine dye bearing carboxylic anchoring group directly substituted in the aromatic ring giving photoconversion efficiency of 4.5% with photon harvesting up to 700 nm. Such an efficiency given by squaraine sensitizer broke the myth about the poor power conversion efficiency of squaraine dyes reported by various research groups [9–11]. A perusal of squaraine based sensitizers bearing carboxyl anchoring group clearly corroborates that dyes bearing carboxylic group directly substituted to aromatic ring are superior in performance as compared to that of their alkyl side chain carboxy substituted counterparts. This has been explained by the strong conjugation across the chromophoric main body and anchoring group leading to good electronic coupling between the lowest unoccupied molecular orbital (LUMO) of the sensitizer and conduction band of TiO_2. This work ignited the more intense research for this class of dyes leading towards the further improvement in efficiency by fabrication of hybrid DSSCs using squaraine dyes with other sensitizers [12–14].

Amongst the squaric acid based dyes bearing ring substituted carboxyindoles, there are scattered reports about the selection and suitability of the alkyl substituents at N-position of the indole ring. Although, Yum et al. [8] have used octyl indole while Chen et al. [15] have used the butyl indole. There is no discussion about the reason for the selection of a particular alkyl group substituted at

* Corresponding author. Tel.: +81 93 695 6044; fax: +81 93 695 6005.
E-mail address: shyam@life.kyutech.ac.jp (S.S. Pandey).

1010-6030/$ – see front matter © 2010 Elsevier B.V. All rights reserved.
doi:10.1016/j.jphotochem.2010.07.010

N-position of the indole ring in their investigation. In this regard, Sayama et al. [16] have although advocated the importance of long alkyl substituents towards the enhancement of photoconversion efficiency but their report was mainly focused on merocyanine dyes absorbing effectively in lower wavelength region. In the present investigation, we would like to report our systematic study of role of substituents on the sensitization behavior of model squaraine dyes bearing variable alkyl chain length as well as fluoroalkyl substituent. Results of the cell performance have been elucidated using dark current–voltage (*I–V*) characteristics, extent of dye adsorption, dye surface potential, electron life-time and electron diffusion length measurements. At the same time novelty also lies in the fact that role of substituent on controlling the HOMO and LUMO of the squaraine dyes which is helpful for the design and development of novel NIR sensitizers.

2. Experimental

2.1. Materials, instruments and methods

1-Iodoethane (**2**), 1-iodobutane (**3**), 1-iodooctane (**4**), 1-iodododecane (**5**), 1-iodooctadecane (**6**) and 1,1,1-trifluoro-4-iodobutane (**7**) used in the present synthesis were purchased from Tokyo Kasei Co. Ltd. Solvents (reagent grade, Wako Chemical Company) and squaric acid were purchased from Alfa Aesar and used as received. Synthesized squaraine (**SQ**) dyes and dye intermediates were analyzed by high performance liquid chromatography (JASCO) equipped with ODS analytical column (CD-C18, ϕ 4.6 mm × 150 mm) and UV as well as multi channel photodiode array detector for monitoring the reaction progress and final purity of the compound.

Mass of the intermediates as well as final SQ dyes was confirmed by MALDI-TOF-mass (Applied Biosystems) or fast ion bombardment (FAB) mass in positive ion monitoring mode. For final SQ dyes, high resolution FAB-mass (HR-MS) in positive ion monitoring mode was also measured. Nuclear magnetic resonance (NMR) spectra were recorded on a JEOL JNM A500 MHz spectrometer in $CDCl_3$ or d_6-DMSO with reference to TMS for structural elucidation. Electronic absorption spectroscopic investigations in solution and thin film adsorbed on TiO_2 surface were conducted using UV–vis spectrophotometer (JASCO V 550). Surface potential measurement of SQ dyes was performed using scanning Kelvin probe microscope (SKPM model JSPM 5200, JEOL Datum). Surface potential of bare TiO_2 surface was first measured and its value was taken as reference followed by measurement of surface potential of dye adsorbed on TiO_2 film.

Electron diffusion length (L_n) and electron life-time (t_n) of SQ dyes adsorbed on TiO_2 layer were estimated with intensity modulated photocurrent/photovoltage spectroscopic (IMPS/IMVS) measurements [17–19]. The amount of dye molecules adsorbed on TiO_2 layers was measured spectrophotometrically after desorption of adsorbed dye molecules using NaOH aqueous solution and standard calibration curve of respective SQ dye. Optical absorption at λ_{max} was used for the standard calibration curve and calculation of the number of dye molecules quantitatively. Highest occupied molecular orbital (HOMO) energy level of the squaraine dyes used in the present investigation has been determined by photoelectron spectroscopy in air (PESA model AC3) from Riken Keiki Co. Ltd. Japan while their lowest unoccupied molecular orbital (LUMO) energy level was determined from the edge of optical absorption using electronic absorption spectroscopy.

2.2. Synthesis of SQ dyes and dye intermediates

Aromatic ring carboxy functionalized indole derivative 2,3,3-trimethyl-3H-indole-5-carboxylic acid was synthesized following the methodology reported by Pham et al. [20]. Symmetrical SQ dyes and corresponding dye intermediates of 5-carboxy-2,3,3-trimethyl-indole have been synthesized following the methodology as shown in Scheme 1.

2.2.1. Synthesis of 2,3,3-trimethyl-3H-indole-5-carboxylic acid [*1*]

In a round bottom flask fitted with condenser and N_2 purging, 4-hydrazinobenzoic acid (5.0 g; 32.85 mmol), glacial acetic acid (80 ml) + sodium acetate (5.5 g; 67 mmol) + 3-methyl-2-butanone (4.45 g; 51.5 mmol) were added. Reaction mixture was refluxed at 120 °C for 8 h leading to brown suspension. Acetic acid was evaporated followed by addition of 9:1 water methanol mixture on ice-bath leading to precipitation. Residue was filtered and dried giving 3.7 g of titled compound as off white powder in 56% yield. HPLC analysis of product suggests that compound was 100% pure. FAB-mass (measured 203; calculated 203.09) and ^{1}H NMR (500 MHz, $CDCl_3$): d/ppm = 7.99 (s, H-4), 7.93 (d, J = 8.0 Hz, H-6), 7.59 (d, J = 8.0 Hz, H-7), 2.26 (s, 3H, H-10), 1.28 (s, 6H, H11 + 12) verifies the successful synthesis of the compound.

2.2.2. Synthesis of 5-carboxy-2,3,3-trimethyl-1-alkyl-3H-indolium iodide [*8*–*12*]

2,3,3-trimethyl-3H-indole-5-carboxylic acid (**1**, 1 equiv.) and 1-iodoalkane (**2**–**7**, 3 equiv.) were dissolved in dehydrated acetonitrile and reaction mixture was refluxed for (**2**: 24 h, **3**: 48 h; **4**: 72 h; **5**: 96 h and **6**: 144 h) under nitrogen atmosphere to give corresponding 5-carboxy-N-alkyl-indoium iodides (**8**–**12**). In the case of **7**, reaction was carried at 130 °C for 24 h using propionitrile solvent. After completion of the reaction as monitored by HPLC, solvent was evaporated and the crude product was washed with ample diethyl ether giving the titled compound. The physical and spectral data of N-alkyl-indolium iodides (**8**–**12**) are as follows.

*2.2.2.1. 5-Carboxy-2,3,3-trimethyl-1-ethyl-3H-indolium iodide (**8**).* Yield 79% having 98% purity as confirmed by HPLC. FAB-mass (measured 232.0; calculated 232.13) and ^{1}H NMR (500 MHz, d_6 DMSO): d/ppm = 8.40 (s, H-4), 8.19 (d, J = 8.0 Hz, H-6), 8.08 (d, H = 8.0 Hz, H-7), 4.52 (q, 2H, H-13), 2.87 (s, 3H, H-10), 1.28 (s, 6H, H11 + 12), 1.09 (t, 3H, H-14) confirms the identity of the compound.

*2.2.2.2. 5-Carboxy-2,3,3-trimethyl-1-butyl-3H-indolium iodide (**9**).* Yield 77% having 97% purity as confirmed by HPLC. FAB-mass (measured 260.0; calculated 260.16) confirms successful synthesis of the compound.

*2.2.2.3. 5-Carboxy-2,3,3-trimethyl-1-octyl-3H-indolium iodide (**10**).* Yield 72% having 96% purity as confirmed by HPLC. FAB-mass (measured m/z: 316.0; calculated m/z: 316.23) confirms successful synthesis of the compound.

*2.2.2.4. 5-Carboxy-2,3,3-trimethyl-1-dodecyl-3H-indolium iodide (**11**).* Yield 66% having 98% purity as confirmed by HPLC. FAB-mass (measured 372.0; calculated 372.29) confirms the identity of the compound.

*2.2.2.5. 5-Carboxy-2,3,3-trimethyl-1-octadecyl-3H-indolium iodide (**12**).* Yield 56% having 98% purity as confirmed by HPLC. MALDI-TOF-mass (measured 456.69; calculated 456.38) confirms the successful synthesis of the compound.

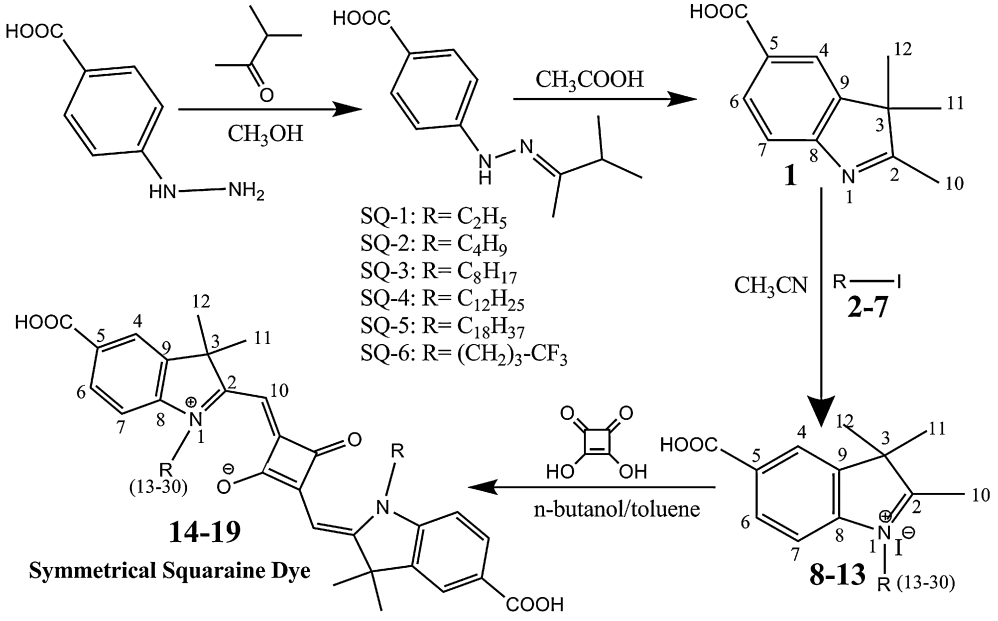

Scheme 1. Synthesis of symmetrical squaraine dyes.

*2.2.2.6. 5-Carboxy-2,3,3-trimethyl-1-Trifluorobutyl-3H-indolium iodide (**13**).* Yield 46% having 99% purity as confirmed by HPLC. FAB-mass (measured 441.0; calculated 441.04) confirms the successful synthesis of the compound.

*2.2.3. Synthesis of symmetrical squarine dyes [**14**–**19**]*

Symmetrical SQ Dyes (**SQ-1**–**6**) were synthesized using corresponding carboxy functionalized trimethyl-indolium iodide salt **8**–**13** ((2 equiv.) and squaric acid (1 equiv.) in 1-butanol:toluene mixture (1:1, v/v). Reaction mixture was refluxed for 18 h using Dean–Stark trap for azeotropic removal of water. After completion of reaction, reaction mixture was cooled, solvent was evaporated and product was purified by silica gel column chromatography using chloroform: methanol as eluting solvent. The physical and spectroscopic data of symmetrical SQ dyes are as follows;

*2.2.3.1. N-ethyl substituted squarine dye **SQ-1** (**14**).* Yield 58% and HPLC purity 98%. MALDI-TOF-mass (calculated 540.22 and observed 541.49 $[M+H]^+$). HR-MS (calculated 540.226 and observed 540.223 $[M]^+$). ^{1}H NMR (500 MHz, d_6-DMSO): d/ppm = 8.04 (dd, H-6), 7.98 (dd, H-4), 7.42 (dd, H-7), 5.89 (s, H-10), 4.17 (q, 2H, H-13), 1.71 (s, 6H, H11 + 12), 1.30 (t, 3H, H-14) confirms the successful synthesis of the dye SQ-1.

*2.2.3.2. N-butyl substituted squarine dye **SQ-2** (**15**).* Yield 64% and HPLC purity 98%. MALDI-TOF-mass (calculated 596.29 and observed 597.25 $[M+H]^+$). HR-MS (calculated 596.288 and observed 596.296 $[M]^+$). ^{1}H NMR (500 MHz, d_6-DMSO): d/ppm = 12.85 (b, –COOH), 8.04 (dd, H-6), 7.96 (dd, H-4), 7.43 (dd, H-7), 5.90 (s, H-10), 4.13 (q, 2H, H-13), 1.76 (m, 2H, H-14), 1.70 (s, 6H, H11 + 12), 1.40 (m, 2H, H-15), 0.95 (t, 3H, H-16) confirms the successful synthesis of the dye **SQ-2**.

*2.2.3.3. N-octyl substituted squarine dye **SQ-3** (**16**).* Yield 46% and HPLC purity 97%. MALDI-TOF-mass (calculated 708.41 and observed 708.48 $[M]^+$). HR-MS (calculated 708.413 and observed 708.412 $[M]^+$). ^{1}H NMR (500 MHz, d_6-DMSO): d/ppm = 12.84 (b, –COOH), 8.04 (dd, H-6), 7.96 (dd, H-4), 7.43 (dd, H-7), 5.90 (s, H-10), 4.1 (q, 2H, H-13), 1.70 (s, 6H, H11 + 12), 1.40–1.20 (m, 12H, H-14 to H-19), 0.83 (t, 3H, H-20) confirms the successful synthesis of the dye **SQ-3**.

*2.2.3.4. N-dodecyl substituted squarine dye **SQ-4** (**17**).* Yield 55% and HPLC purity 98%. MALDI-TOF-mass (calculated 820.54 and observed 821.84 $[M+H]^+$). HR-MS (calculated 820.539 and observed 820.537 $[M]^+$).

*2.2.3.5. N-octadecyl substituted squarine dye **SQ-5** (**18**).* Yield 64% and HPLC purity 98%. MALDI-TOF-mass (calculated 988.73 and observed 989.40 $[M+H]^+$). HR-MS (calculated 988.727 and observed 989.0000 $[M]^+$).

*2.2.3.6. N-Trifluorobutyl substituted squarine dye **SQ-6** (**19**).* Yield 71% and HPLC purity 99%. FAB-mass (calculated 704.23 and observed 705.0 $[M+H]^+$) confirms the identity of the compound.

2.3. DSSC fabrication and measurement of solar cell performance

DSSC were fabricated using Ti-Nanoxide D paste (Solaronix SA) which was coated on a Low E glass (Nippon Sheet Glass Co., Ltd.) by a doctor-blade. The substrate was then baked at 450 °C to fabricate TiO_2 layers of about 12 μm thickness. The substrate was dipped in the solution containing dye in the presence and/or absence of CDCA. The dye concentration was fixed to be 0.25 mM while CDCA concentration was 2.5 mM. A Pt sputtered SnO_2/F glass substrate was employed as the counter electrode. Electrolyte (WWS30) containing LiI (500 mM), iodine (50 mM), t-butylpyridine (580 mM), MeEtImDCA (ethylmethylimidazolium dicyanoimide) (4:6 w/w) (600 mM) in acetonitrile, was used to fabricate the DSSC. A Himilan film (Mitsui-DuPont Polychemical Co., Ltd.) of 25 μm thickness was used as a spacer. The cell area was 0.25 cm^2. Solar cells were evaluated by using a photo-mask on the solar cell in order to remove the effect of the optical reflection under the irradiation of 100 mW/cm^2 at AM 1.5. No special efforts were made towards cell optimization such as, electrode ($TiCl_4$ treatment, use of scattering layer) and at electrolyte level in order to attain the maximum possible efficiency. Photoconversion efficiencies were calculated without the correction incorporated pertaining

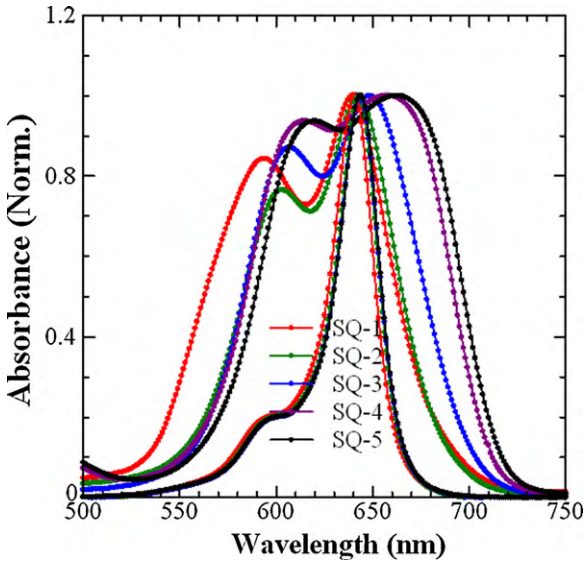

Fig. 1. Absorption spectra of symmetrical squaraines in DMF solution and thin film adsorbed on nanoporous TiO_2 (4 μm).

to the light absorption and reflection caused by conducting glass substrate.

3. Results and discussion

3.1. Electronic absorption of squaraine dyes

UV–vis absorption spectra of squarine dyes in DMF solution as shown in Fig. 1 exhibit a sharp absorption peak at 640–643 nm associated with π–π* electronic transition which undergo spectral broadening and red shift upon adsorption onto thin TiO_2 film and could be attributed to the interaction between carboxyl functionality of squaraine dyes with the titania surface. It is interesting to note that spectral broadening and red shift increases with the increasing alkyl chain length. This can probably be explained by facile J-aggregate formation by squaraine dyes bearing longer alkyl chains due to improved self-aggregation. Similar kind of spectral broadening and red shift in the edge of IPCE as a function of increase in the alkyl chain length have also been observed by Sayama et al. [16].

It is noteworthy to see that **SQ-1** having ethyl substation shows the pronounced blue shift in the absorption spectra along with relatively enhanced lower wavelength shoulder peak and could be attributed to enhanced H-aggregate formation. Kim et al. [21] have also observed the formation of blue shifted H-aggregates formed by squarine dyes on SnO_2 surface absorbing in the lower wavelength region. This lower wavelength absorption is much clearly evident in the IPCE spectrum of **SQ-1** bearing ethyl substituent and is negligible for squaraine dyes having butyl or higher alkyl substituent. This clearly indicates that at least butyl substitution of the carboxy functionalized indole ring at N-position is necessary to suppress the dye aggregation. DFT calculations performed on squaraine dye bearing carboxyl group directly attached to chromophore indicates that HOMO is mainly centralized over squaric acid core while there is sufficient diversion of LUMO over carboxyl moiety along with the indole ring (see Fig. S1) suggesting possibility of facile electron injection from photoexcited dye to TiO_2 conduction band.

3.2. Effect of alkyl chain length of squaraine dyes on DSSC performance

A perusal of the photovoltaic performance of DSSC based on squaraine dyes as shown in Fig. 2 and Table 1 (for table see the supporting information) clearly corroborates that efficiency increases with the increasing alkyl chain length. This increase in the efficiency was associated with increase in both of the Voc as well as Jsc as a function of alkyl chain length. Although variation of alkyl chain length was lacking, Koumura et al. have also advocated the importance of the presence of long alkyl chain in their MK dyes towards efficiency enhancement [22]. They advocated that long alkyl chain not only prevent the approach of the acceptor molecules to the TiO_2 surface but suppress the dye aggregation also, making favorable condition for electron transport.

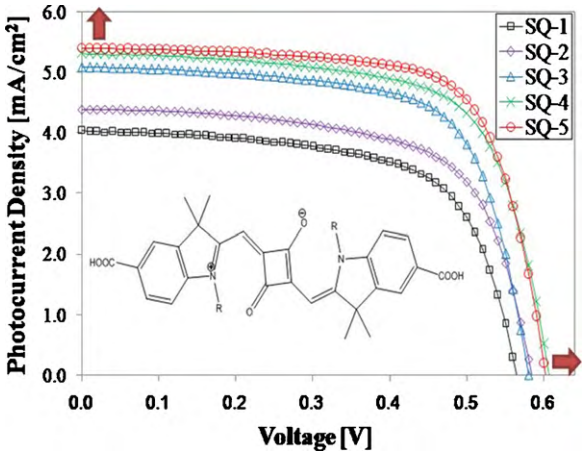

Fig. 2. Photocurrent–voltage characteristics for the DSSC based on squaraine dyes bearing variable alkyl chains (C_2–C_{18}).

3.2.1. Elucidation of Voc increase as a function of alkyl chain length

Enhancement of the Voc as a function of alkyl chain length in these squaraine dyes was elucidated by dark current–voltage (*I–V*) characteristics, electron life-time and surface potential measurements (see Figs. S2–S4 in supporting information). Shift of the onset of dark currents towards higher voltage indicates the suppression of recombination leading to improved Voc for squaraine dyes bearing longer alkyl chains. This was further confirmed by the electron life-time measurement, which increases with increasing alkyl chain length. Using different kind of organic sensitizers Miyashita et al. [23] have also emphasized that organic dye having longer alkyl chain exhibits the increased electron life-time. Recently, Sakaguchi et al. [24] have reported the increase in the Voc with the increase of surface potential for different sensitizer, which was reasoned with the upward shift of the conduction band edge of TiO_2. Surface potential of squaraine dyes was also found to increase with the increasing alkyl chain length (see Fig. S4) and could be, therefore, attributed to the increase in Voc. Fig. 3 exhibits a correlation between electron life-time and Voc for model squaraine dyes and clearly indicates that squaraine dye bearing longer alkyl chain exhibits higher Voc due to longer electron life-time. It also suggests that dodecyl alkyl chain length is optimum for attaining the highest observed Voc.

3.2.2. Elucidation of Jsc improvement as a function of alkyl chain length

Enhancement of Jsc was elucidated with incident photon to electron conversion efficiency (IPCE), electron diffusion length (Fig. S5) and extent of dye adsorption on the TiO_2 surface (Fig. S6). With the increasing alkyl chain length, spectral broadening of IPCE along with its increase can be attributed to the enhanced Jsc as a function of increasing alkyl chain length as shown in Fig. 4. Increase in the Jsc was also found to be in accordance with the increased electron diffusion length in the case

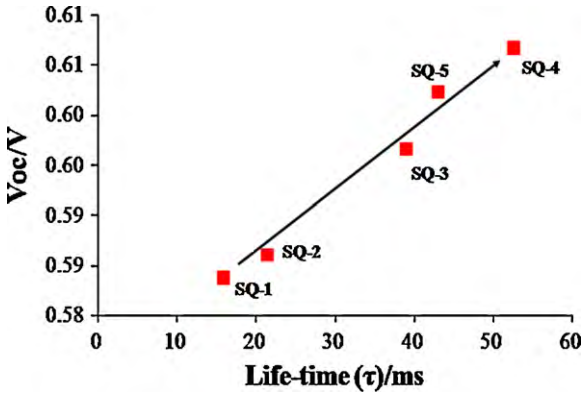

Fig. 3. Relationship between measured electron life time and observed Voc for DSSC based on squaraine dyes having variable alkyl chain length.

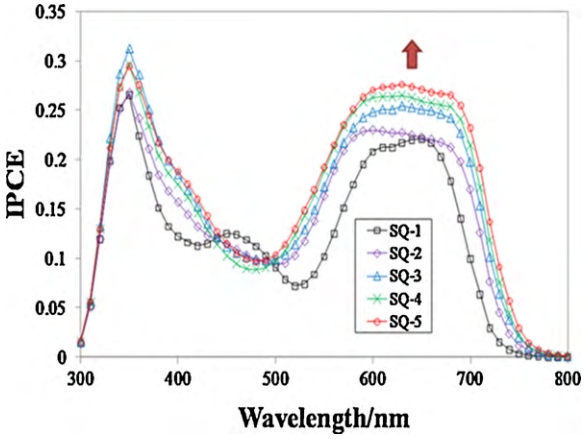

Fig. 4. Photocurrent action spectra of monochromatic incident photon-to-current conversion efficiency for DSSC based on squaraine dyes.

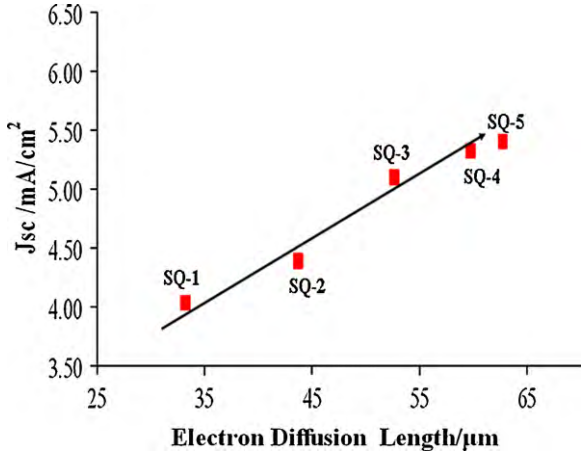

Fig. 5. Correlation between measured electron diffusion length and Jsc for DSSC based on alkyl substituted model squaraine dyes.

of squaraines bearing longer alkyl chains. Recently, Ogomi et al. [25] have demonstrated that increase in the extent of adsorbed dyes on TiO_2 surface leads to enhanced surface trap passivation resulting in to increased Jsc. It is interesting to note that the extent of the dye adsorbed on TiO_2 surface increases with the increasing alkyl chain length which supports the increased Jsc for squaraine dyes having longer alkyl chain length. A perusal of Fig. 5 clearly corroborates that squaraine dyes bearing longer alkyl chain length exhibits increased Jsc owing to longer electron diffusion

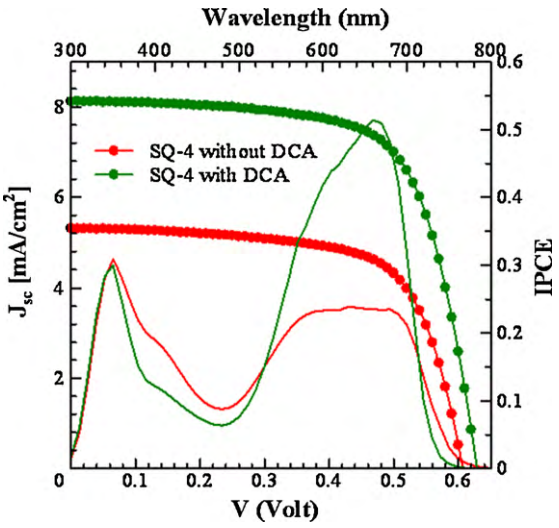

Fig. 6. Effect of CDCA addition on the photovoltaic performance of **SQ-4**. Thin solid line (action spectra) while line with symbol represents the *I–V* curve.

length which ultimately results in to enhanced conversion efficiency.

3.3. Effect of chenodeoxycholic acid as co-adsorbent on DSSC performance

Chenodeoxycholic acid (CDCA) has been widely employed as co-adsorbent along with the sensitizers for the enhancement of efficiency of DSSC owing to its ability to suppress the electron recombination by disrupting the π-aggregates usually formed by squaraine and other organic dyes[24,26]. We employed the CDCA with one of our squaraine dye **SQ-4** to fabricate DSSC which results into pronounced improvement in both of the IPCE and efficiency as shown in Fig. 6. In the presence of CDCA, IPCE of **SQ-4** shows an enhancement from 27% (without CDCA) to 51% having onset of IPCE edge at about 745 nm. In an attempt towards the search for efficient NIR dye, Cid et al. [14] have reported novel unsymmetrical phthalocyanine dye having onset of IPCE edge of about 725 nm giving power conversion efficiency of 3.5%. **SQ-4** in the presence of CDCA gave a Jsc of 8.12 mA/cm^2, Voc of 0.63 and a fill factor (ff) of 0.69 corresponding to overall power conversion efficiency of 3.53% under global AM 1.5 condition. We would like to mention here that using our model squarine sensitizers, DSSC performance have not yet been optimized in terms TiO_2 surface treatment using $TiCl_4$, most suitable electrolyte and use of scattering layer on to the nanoporous TiO_2 layer. Such optimizations are certainly expected to lead in to further enhancement in power conversion efficiency.

3.4. Effect of substituent on HOMO and LUMO: implication on new dye design

To design a novel sensitizer for DSSC a judicious control of energy level of HOMO and LUMO of dye with respect to the energy level of I_3^-/I^- redox couple and conduction band of TiO_2, respectively, is highly desired. Suitability of a particular dye for NIR sensitization depends on the minimization of energy gap for electron injection to TiO_2 and energy required for dye regeneration. We have also synthesized a new symmetrical squaraine dye **SQ-6** having trifluoro-butyl substitution (Fluoro substituted analogue of **SQ-2**). DSSC fabricated with this dye gave a Jsc of 6.63 mA/cm^2, Voc of 0.57 and a fill factor (ff) of 0.70 corresponding to the overall power conversion efficiency of 2.65% under global AM 1.5 condition (see

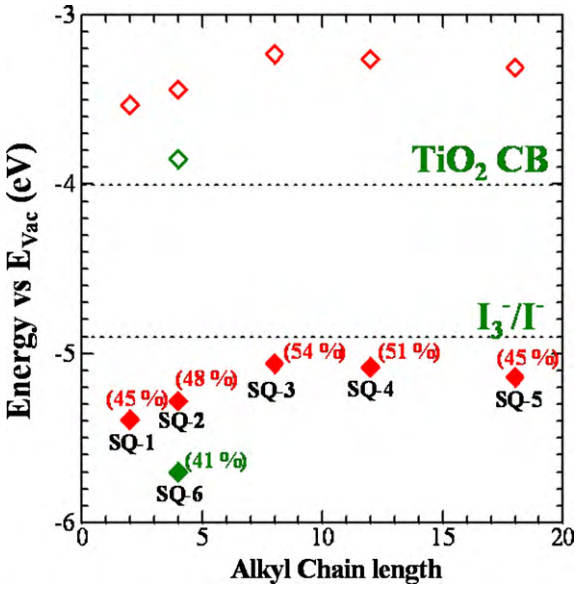

Fig. 7. HOMO and LUMO energy level of squaraine dyes used in the present investigation. Values in parentheses represent the maximum IPCE for the DSSC based on dyes under investigation.

Fig. S6 for *I–V* characteristics and IPCE in the supporting information). Redox potential of I_3^-/I^- redox couple has been reported to be 0.44 V vs. NHE [27] which can be translated into −4.9 eV with respected to the vacuum level as shown in Fig. 7 by dotted line. Conduction band (CB) of TiO_2 was considered as –4.0 eV considering the most negative quasi Fermi level corresponds to the flat band potential of TiO_2 (0.7 V vs. SCE) as reported by Ogomi et al. [28]. For the normal DSSC operation, there should be finite energy gap between the LUMO of dye and CB of TiO_2 for electron injection as well as HOMO of the dye and redox potential of I_3^-/I^- for dye regeneration after photo-excitation of the dye. Information about this energy barrier is expected to help for the design of novel sensitizers having absorption in longer wavelength region. The HOMO and LUMO energy levels of SQ dyes used in the present investigation have been shown in Fig. 7 which clearly indicates that these energy level for symmetrical squaraine dyes increase with the increasing alkyl chain length up to octyl substituent while fluorine substitution leads to a drastic decrease in the energy of both of the energy level. The HOMO energy level of **SQ-3** having octyl chain substituent has been estimated to be −5.06 eV using AC3 measurement which is about 0.16 eV below the energy level of the redox couple. IPCE for DSSC based on this dye at its absorption maximum (54%) indicates that even at this energy barrier dye is getting successfully regenerated after photo-excitation.

LUMO level of the SQ dyes as shown in Fig. 7 was estimated by the relation $E_{LUMO} = E_{HOMO} - E_g$, where, E_{LUMO}, E_{HOMO} and E_g are LUMO energy level, HOMO energy level and band gap of the dye molecule under investigation, respectively. E_g was estimated from the optical absorption edge using the electronic absorption spectroscopy. As indicated from the figure that lowest LUMO level (−3.84 eV) was observed for **SQ-6** having the Trifluorobutyl substituent. Observation of the LUMO energy level of **SQ-6** above 0.16 eV from the CB of TiO_2 and observation of 41% IPCE at absorption maximum of the dye suggests that even at such an energy barrier electron injection from the photoexcited dye to the CB of TiO_2 is possible. Therefore, maximum HOMO and minimum LUMO energy level of **SQ-3** and **SQ-6** amongst the dyes used in the present work, clearly corroborates that an energy barrier of about 0.16 eV seems to be sufficient for dye regeneration after photo excitation and electron injection to TiO_2 CB in DSSC based on TiO_2 anode and I_3^-/I^- redox system, respectively. Taking this into consideration it is, therefore, possible to design a dye sensitizer having an energy gap of about 1.3 eV [0.9 eV (TiO_2-redox couple energy gap) + 0.4 eV (energy barrier for electron injection and dye regeneration)] i.e. photon harvesting up to 950 nm. Thus it possible to design a novel NIR sensitizer by judicious selection of aromatic moieties surrounding the squaraine core while control of HOMO and LUMO energy level can be made by suitable alkyl or fluoro alkyl substituents.

4. Conclusion

In conclusion, role of alkyl chain length towards the enhancement of photoconversion efficiency of DSSC based on NIR wavelength absorbing squaraine dyes has been demonstrated. Our results indicate that alkyl chain length more than butyl is necessary to prevent the dye aggregation and dodecyl alkyl substituent was found to be optimum giving highest Voc. We would like to emphasize that model squaraine dyes having longer alkyl chain exhibit the enhanced adsorption of dyes on TiO_2 surface leading to better passivation of surface traps. Enhanced surface passivation leads to increase in the electron life-time and electron diffusion length resulting in to increase in the observed Voc and Jsc, respectively. Measurement of HOMO and LUMO of model squaraine dyes used in the present investigation reveal that it possible to design novel squaraine dyes having photon harvesting up to 950 nm by judicious selection of alkyl and fluoroalkyl substituents along with aromatic moieties around squaric acid core.

Acknowledgement

Authors would like to acknowledge the financial support from the New Energy Industrial Technology Development Organization (NEDO), Japan

Appendix A. Supplementary data

Supplementary data associated with this article can be found, in the online version, at doi:10.1016/j.jphotochem.2010.07.010.

References

[1] M.K. Nazeeruddin, F. De Angelis, S. Fantacci, A. Selloni, G. Viscardi, P. Liska, S. Ito, B. Takeru, M. Gratzel, Combined experimental and DFT-TDDFT computational study of photoelectrochemical cell ruthenium sensitizers, J. Am. Chem. Soc. 127 (2005) 16835–16847.
[2] M. Gratzel, Solar energy conversion by dye-sensitized photovoltaic cells, Inorg. Chem. 44 (2005) 6841–6851.
[3] Y. Noma, K. Iizuka, Y. Ogomi, S.S. Pandey, S. Hayase, Preparation of double dye-layer structure of dye-sensitized solar cells from cocktail solutions for harvesting light in wide range of wavelengths, Jpn. J. Appl. Phys. 48 (2009) 020213.
[4] F. Inakazu, Y. Noma, Y. Ogomi, S. Hayase, Dye-sensitized solar cells consisting of dye-bilayer structure stained with two dyes for harvesting light of wide range of wavelength, Appl. Phys. Lett. 93 (2008) 93304.
[5] K.Y. Law, F.C. Bailey, Squarine chemistry-synthesis, characterization and optical properties of a class of novel unsymmetrical squarines—4-(dimethylamino)-phenyl (4′-methoxyphenyl)-squarine and its derivatives, J. Org. Chem. 57 (1992) 3278–3286.
[6] K.Y. Law, Organic photoconductive materials—recent trends and developments, Chem. Rev. 93 (1993) 449–486.
[7] S. Sreejith, P. Carol, P. Chithra, A. Ajayaghosh, Squaraine dyes: a mine of molecular materials, J. Mater. Chem. 18 (2008) 264–274.
[8] J.H. Yum, P. Walter, S. Huber, D. Rentsch, T. Geiger, F. Nuesch, F. De Angelis, M. Gratzel, M.K. Nazeeruddin, Efficient far red sensitization of nanocrystalline TiO_2 films by an unsymmetrical squaraine dye, J. Am. Chem. Soc. 129 (2007) 10320–10321.
[9] N. Takeda, B.A. Parkinson, Adsorption morphology, light absorption, and sensitization yields for squaraine dyes on SnS_2 surfaces, J. Am. Chem. Soc. 125 (2003) 5559–5571.
[10] S. Alex, U. Santhosh, S. Das, Dye sensitization of nanocrystalline TiO_2: enhanced efficiency of unsymmetrical versus symmetrical squaraine dyes, J. Photochem. Photobiol. A 172 (2005) 63–71.

[11] X. Chen, J. Guo, X. Peng, M. Guo, Y. Xu, L. Shi, S.C. Liang, L. Wang, Y. Guo, S. Sun, S. Cai, Novel cyanine dyes with different methine chains as sensitizers for nanocrystalline solar cell, J. Photochem. Photobiol. A 171 (2005) 231–236.
[12] J.H. Yum, S.R. Jang, P. Walter, T. Geiger, F. Neusch, S. Kim, J. Ko, M. Gratzel, M.K. Nazeeruddin, Efficient co-sensitization of nanocrystalline TiO_2 films by organic sensitizers, Chem. Commun. (2007) 4680–4682.
[13] H. Choi, S. Kim, S.O. Kang, J. Ko, M.S. Kang, J.N. Clifford, A. Forneli, E. Palomares, M.K. Nazeeruddin, M. Gratzel, Stepwise cosensitization of nanocrystalline TiO_2 films utilizing Al_2O_3 layers in dye-sensitized solar cells, Angew. Chem. 120 (2008) 8383–8387.
[14] J.J. Cid, J.H. Yum, S.R. Jang, M.K. Nazeeruddin, E.M. Ferrero, E. Palomares, J. Ko, M. Gratzel, T. Torres, Molecular cosensitization for efficient panchromatic dye-sensitized solar cells, Angew. Chem. Int. Ed. 46 (2007) 8358–8362.
[15] Y.S. Chen, Z.H. Zeng, C. Li, W.B. Wang, X.S. Wang, B.W. Zhang, Highly efficient co-sensitization of nanocrystalline TiO_2 electrodes with plural organic dyes, New J. Chem. 29 (2005) 773–776.
[16] K. Sayama, S. Tsugakoshi, K. Hara, Y. Ohga, A. Shinpou, Y. Abe, S. Suga, H. Arakawa, Photoelectrochemical properties of j aggregates of benzothiazole merocyanine dyes on a nanostructured TiO_2 film, J. Phys. Chem. B 106 (2002) 1363–1371.
[17] G. Schlichthörl, S.Y. Huang, J. Sprague, A.J. Frank, Band edge movement and recombination kinetics in dye-sensitized nanocrystalline TiO_2 solar cells: a study by intensity modulated photovoltage spectroscopy, J. Phys. Chem. B 101 (1997) 8141–8155.
[18] L.M. Peter, K.G.U. Wijayantha, Electron transport and back reaction in dye sensitised nanocrystalline photovoltaic cells, Electrochim. Acta 45 (2000) 4543–4551.
[19] T. Yoshida, T. Oekermann, K. Okabe, D. Schlettwein, K. Funabiki, H. Minoura, Cathodic electrodeposition of ZnO/EosinY hybrid thin films from dye added zinc nitrate bath and their photoelectrochemical characterizations, Electrochemistry 70 (2002) 470.
[20] W. Pham, W.F. Lai, R. Weissleder, C.H. Tung, High efficiency synthesis of a bioconjugatable near-infrared fluorochrome, Bioconjug. Chem. 14 (2003) 1048–1051.
[21] Y.S. Kim, K.N. Liang, K.Y. Law, D.G. Whitten, An investigation of photocurrent generation by squarine aggregates in monolayer modifies SnO_2 electrodes, J. Phys. Chem. 98 (1994) 984–988.
[22] N. Koumura, Z.S. Wang, S. Mori, M. Miyashita, E. Suzuki, K. Hara, Alkyl-functionalized organic dyes for efficient molecular photovoltaics, J. Am. Chem. Soc. 128 (2006) 14256–14257.
[23] M. Miyashita, K. Sunahara, T. Nishikawa, Y. Uemura, N. Koumura, K. Hara, A. Mori, T. Abe, E. Suzuki, S. Mori, Interfacial electron-transfer kinetics in metal-free organic dye-sensitized solar cells: combined effects of molecular structure of dyes and electrolytes, J. Am. Chem. Soc. 130 (2008) 17874–17881.
[24] S. Sakaguchi, S.S. Pandey, K. Okada, Y. Yamaguchi, S. Hayase, Probing TiO_2/Dye interface in dye sensitized solar cells using surface potential measurement, Appl. Phys. Exp. 1 (2008) 105001.
[25] Y. Ogomi, Y. Kashiwa, Y. Noma, Y. Fujita, S. Kojima, M. Kono, Y. Yamaguchi, S. Hayase, photovoltaic performance of dye-sensitized solar cells stained with black dye under pressurized condition and mechanism for high efficiency, Sol. Energy Mater. Sol. Cells vol.93 (2009) 1009–1012.
[26] K. Hara, Y. Dan-oh, C. Kasada, Y. Ohga, A. Shinpo, S. Suga, K. Sayama, H. Arakawa, Effect of additives on the photovoltaic performance of coumarin-dye-sensitized nanocrystalline TiO_2 solar cells, Langmuir 20 (2004) 4205–4210.
[27] A. Hagfeldt, M. Gratzel, Light induced redox reactions in nanocrystalline systems, Chem. Rev. 95 (1995) 49–68.
[28] Y. Ogomi, T. Kato, S. Hayase, Dye sensitized solar cells consisting of ionic liquids and solidification, J. Photopylm. Sci. Technol. 19 (2006) 403–408.